

# Comparison of the quantum and classical calculations of flux density of (220) channeled positrons in Si crystal

K B Korotchenko<sup>1</sup>, T A Tukhfatullin<sup>1</sup>, Yu L Pivovarov<sup>2</sup> and Yu L Eikhorn<sup>1</sup>

<sup>1</sup>National Research Tomsk Polytechnic University, 30 Lenin Avenue, 634050 Tomsk, Russia

<sup>2</sup>V.E. Zuev Institute of Atmospheric Optics SB RAS, 1 Zuev Square. 634034 Tomsk, Russia

E-mail: aihorniyurij@mail.ru

**Abstract.** Simulation of flux-peaking effect of the 255 MeV positrons channeled in (220) Si crystals is performed in the frame of classical and quantum mechanics. Comparison of the results obtained using both approaches shows relatively good agreement.

## 1. Introduction

The flux-peaking effect (FPE) is one of the known orientation effects at channeling of positively charged particles. A detailed review of the FPE was given in [1]. Theoretical investigation of the FPE has been carried out on the basis of kinetic equations for the particle distribution functions or numerical solution of classical equation of motion [2]. In this work we perform analysis of FPE using both classical and quantum methods as in work [3]. We use computer code “Basic Channeling with Mathematica<sup>®</sup>” BCM-1.0 [4], which was successfully applied to describe recent theoretical [5-10] and experimental results [11-15], obtained at SAGA Light Source. Calculations were performed for 255 MeV positrons channeled along (220) planes in a thin Si crystal.

## 2. Classical description

For the calculation of every individual charged particles trajectory it is necessary to solve classical equation of motion. Under the channeling condition the longitudinal component of relativistic particles velocity  $v_{\parallel}$  is nearly equal to the speed of light  $c$ . The transversal component of velocity is much less than the longitudinal one:  $v_{\perp} \equiv \dot{x} \ll v_{\parallel}$ ;  $v_{\perp}/c \ll 1/\gamma$  ( $\gamma$  denotes the relativistic factor). Thus, equations of motion are reduced to the non-relativistic equation with the replacement of the particle mass  $m$  to the relativistic mass  $\gamma m$ :

$$\gamma m \ddot{x} = -\frac{\partial U(x)}{\partial x}, \quad \gamma m \ddot{z} = 0, \quad (1)$$

Where  $x$  is the transversal coordinates,  $z$  the longitudinal coordinate,  $U(x)$  here describes the potential energy of the particles in the field of periodically arranged crystal planes.

The initial conditions for this system contain the positron entrance point into the crystal  $x(0) \equiv x_0$  and transversal components of initial velocity:



$$v_x(0) = c \sqrt{1 - \frac{1}{\gamma^2}} \sin(\theta), \quad (2)$$

where  $\theta$  is the incidence angle i.e. the angle between positron momentum and channeling plane. The point of entry of particles were uniformly distributed within a period of change the function  $U(x)$  (within one potential well). For the numerical simulation of the equation (1) we use computer code “Basic Channeling with Mathematica©” BCM–1.0 [4]. This code computes numerical solutions of the classical equations of relativistic particles using the Doyle-Turner potential for the crystallographic planes [9]. Simulated trajectories of 255-MeV positrons in 5 $\mu\text{m}$  Si crystal and potential energy of positrons in the (220) crystal planes electric field are shown in figure 1. Only 50 trajectories are presented. The incidence angles for all positrons are the same.

To simulate the angular divergence of positron beam the procedure described in Ref. [5] is used. For each point of entry, 20 values of the incident angle  $\theta$  are generated randomly with a normal distribution. The standard deviation of the distribution had the value 0.1 mrad  $\approx \theta_c/4$  ( $\theta_c$  is the critical channeling angle). Thus, 10 000 trajectories are calculated for different entry points within one period of the planar channeling potential (figure 1(a)). Then, using these trajectories we obtain 2D spatial distribution of the positrons inside the crystal.

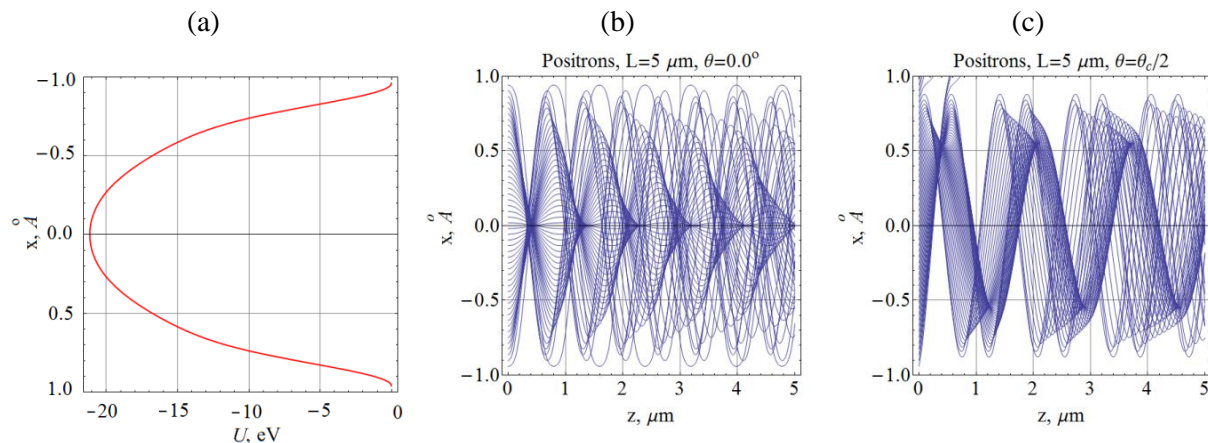


**Figure 1.** Simulated trajectories of 255 MeV positrons in 5 $\mu\text{m}$  Si crystal and potential energy of positrons in the electric field of the crystal planes. (a) (220) interplanar potential energy, (b) 50 simulated trajectories for incidence angle  $\theta=0.0$ , (c) 50 simulated trajectories for incidence angle  $\theta=\theta_c/2$ .

### 3. Quantum description

The channeled particle wave function  $\Phi_i(x)$  was calculated using computer code “Basic Channeling with Mathematica©” BCM–1.0 [4]. This code computes numerical solutions of the Schrödinger equations with relativistic mass [10] for relativistic particles using the Doyle-Turner approximation for the crystallographic planes potential [9].

The conventional wave packet  $\Psi(x,t)$  based on the wave functions  $\Phi_i(x)$  we have chosen as

$$\Psi(x,t,\theta) = \sum_i P_i(\theta) \exp\left(-i \frac{\varepsilon_i}{\hbar} t\right) \Phi_i(x), \quad (3)$$

where  $P_i(\theta)$  is the initial population of the transverse sub-barrier energy levels:

$$P_i(\theta) = \frac{1}{d} \left| \int_{-d/2}^{d/2} \exp(ik_x \theta \cdot x) \Phi_i(x) dx \right|^2. \quad (4)$$

Here  $\theta$  is the positrons initial angle of incidence,  $k_x$  the transverse wave vector component,  $d$  the interplanar distance,  $\varepsilon_i$  the eigenvalues of Schrödinger equation.

In addition, the probability density of positrons wave packet was obtained by analogy with the free particles Gaussian wave packet:

$$\Psi_G(x, t, \theta) = \sum_i \sum_m P_i(\theta) \tilde{\Phi}_{i,m} \exp\left(i m g x - i \frac{\varepsilon_i}{\hbar} t\right), \quad (5)$$

where  $\tilde{\Phi}_{i,m}$  is the Fourier transform of wave function  $\Phi_i(x)$ ,  $g$  reciprocal lattice vector.

#### 4. Results of simulation

The spatial distribution of the 255 MeV positrons channeled in a 5  $\mu\text{m}$  thick Si crystal along (220) planes are shown in figure 2 obtained using classical approach. Left column represents spatial distribution for parallel positron beam. In the right column spatial distributions of positrons inside the crystal for beam with angular divergences are shown. It is clearly seen that number of maximum of spatial distribution equal 6 for crystal thickness 5  $\mu\text{m}$  and angle of incidence  $\theta=0^\circ$  (see, in figure 2(a)).

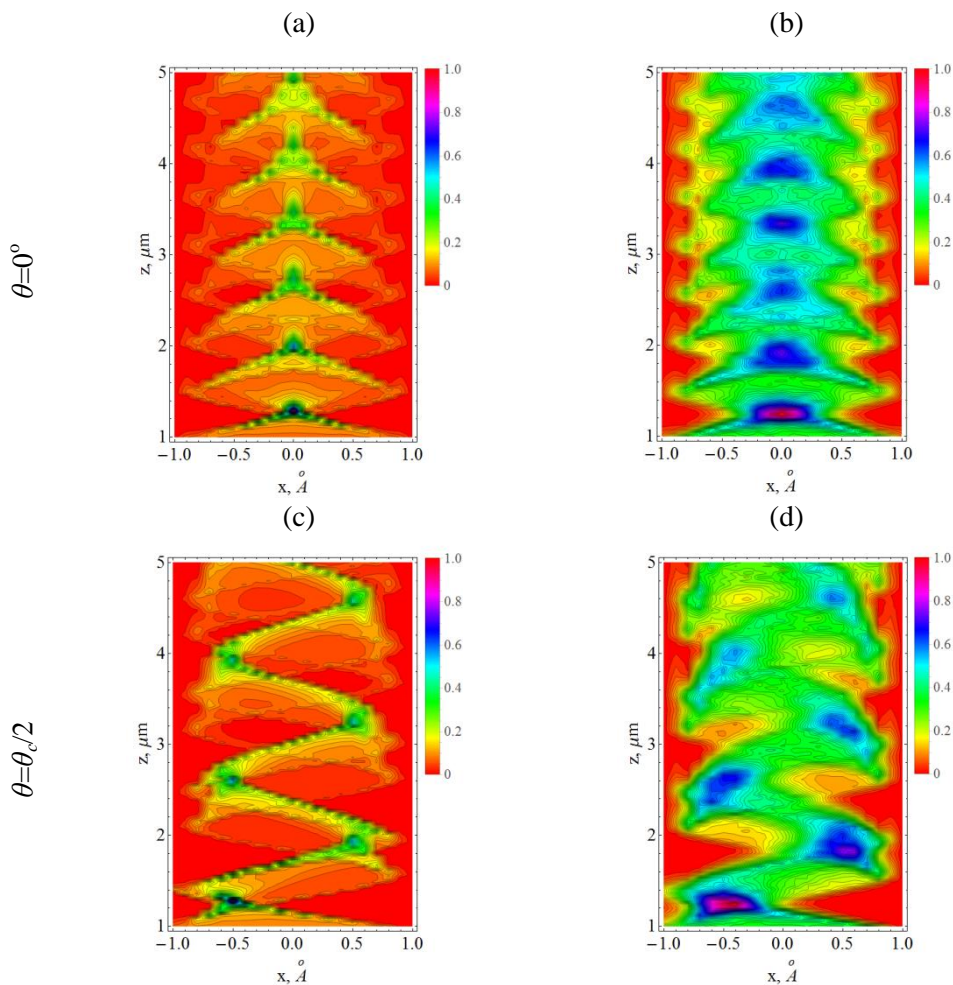


**Figure 2.** Spatial distribution of the 255 MeV positrons channeled in (220) Si crystal for incident angle  $\theta=0^\circ$  and  $\theta=\theta_c/2=0.012^\circ=0.2$  mrad. (a, c) parallel positron beam (no angular divergence), (b, d) beam with angular divergences equals  $0.1$  mrad  $\approx \theta_c/4$ .

For beam with angular divergence the quantity of maximum does not change but it became wider (see, in figure 2(b)). Spatial distributions of positrons for incident angle  $\theta=\theta_c/2$  are shown in figure 2 (c,d). In this case the spatial distribution has specific “zigzag” shape. This is due to the form of positron trajectories which are determined interplanar potential which is close to parabolic (see, in figure 1).

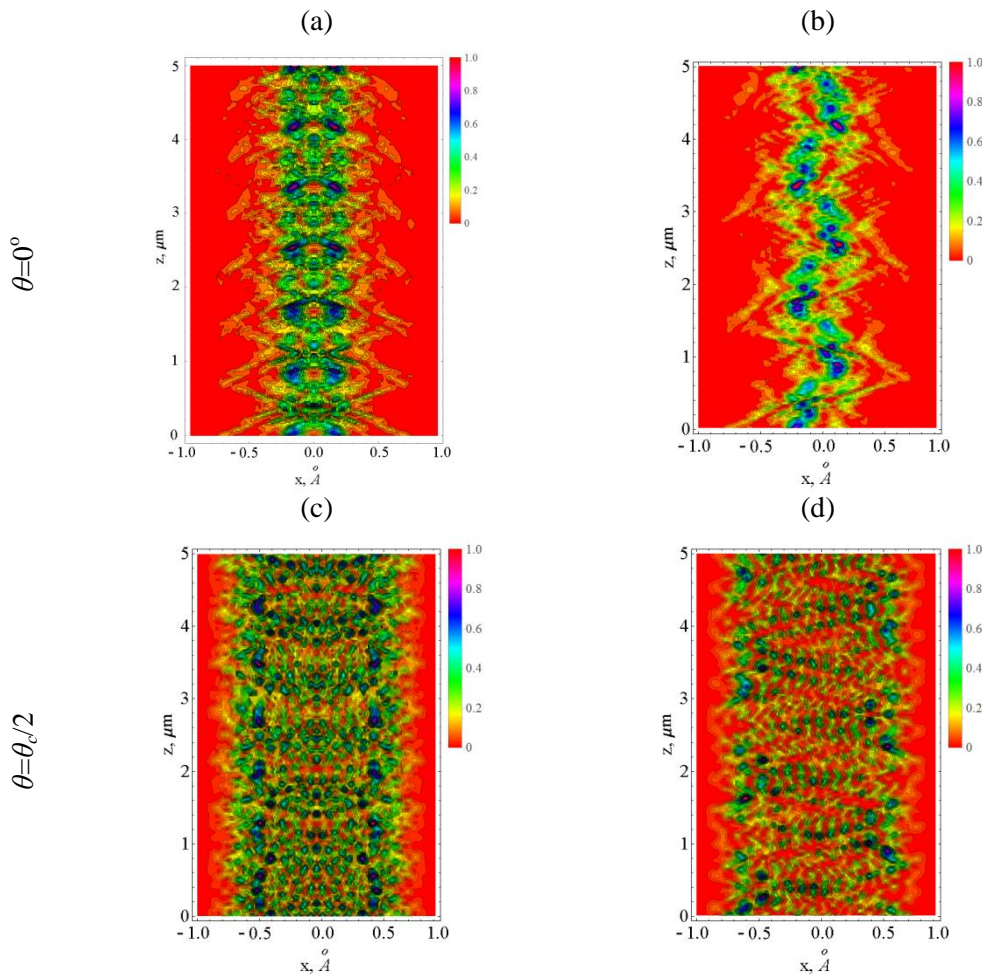


**Figure 3.** Wave packet probability density of the 255 MeV positrons channeled in (220) Si crystal for incident angles  $\theta=0^\circ$  and  $\theta=\theta_c/2$ . (a, c) The conventional wave packet  $\Psi(x,t,\theta)$ ; (b, d) the Gaussian wave packet  $\Psi_G(x,t,\theta)$ .

Probability density of positrons wave packet calculated using formula (4) are shown in figure 3(a,c). The shape of the probability density is more particular than in the case of classical approach but the number of maxima is the same as for classical spatial distribution (see, in figure 2(a)). The probability density of positrons calculated using Gaussian wave packet are shown in figure 3(b, d). It is seen that the form of probability density resembles the classical spatial distribution calculated for incident angle  $\theta = \theta_c/2$ .

## 5. Conclusions

Simulation of flux-peaking effect (FPE) of the 255 MeV positrons channeled in (220) Si crystals is performed in the frame of classical and quantum mechanics using computer code “Basic Channeling with Mathematica©” BCM–1.0. Comparison of the calculation results of the positron beam spatial distribution and the wave packet probability density shows relatively good agreement. This is, mainly, confirms the classical model validity.

However, there are some features: the positron beam “zigzag” shape spatial distribution occurs if angle of incidence is not zero, while a similar distribution for the wave packet probability density occurs only for a Gaussian wave packet. In our opinion, such result means, that the Gaussian wave packet is the most appropriate model of the classical spatial distribution if incident angle of positrons is comparable to the critical angle of channeling.

On the contrary, a good coincidence of classical and quantum results on the flux-peaking effect simulation allows us to conclude that the choice of method is determined by the description of the problem. If we need to estimate the numerical values of the beam parameters, you should use the classic approach. If you need to obtain detailed description of beam spatial distribution, then use the quantum approach.

## 6. Acknowledgements

The reported study was funded by RFBR according to the research project No. 16-32-00464 мол\_a.

## References

1. Kumakhov M A and Shirmer G 1980 *Atomnie stolknovenija v kristallakh (Atomic Collisions in Crystals (in Russian))* (Moscow: Nauka)
2. Dedkov G V, Kumakhov A M and Sokhov M Z 1983 *Radiation Effects* **71** 261
3. Bogdanov O V, Korotchenko K B, Pivovarov Yu L and Tukhfatullin T A 2008 *Nucl. Instrum. & Methods* **B266** 3858
4. Bogdanov O V, Fiks E I, Korotchenko K B, Pivovarov Yu L and Tukhfatullin T A 2010 *J. Phys.: Conf. Ser.* **236** 012029
5. Bogdanov O V, Korotchenko K B, Pivovarov Yu L 2008 *J. Surf. Investigat.* **2**, **2**, 290
6. Bogdanov O V, Korotchenko K B, Pivovarov Yu L 2008 *J. Phys. B: Atomic, Molecular and Optical Physics* **41**, 055004
7. Korotchenko K B 2010 *J. Surf. Investigat.* **4**, **4**, 599
8. Korotchenko K B, Pivovarov Yu L, Tukhfatullin T A 2011 *Nucl. Instrum. & Methods* **B269** 2840
9. Korotchenko K B, Pivovarov Yu L 2014 *J. Phys.: Conf. Ser.* **517** 012019
10. Korotchenko K B and Pivovarov Yu L 2015 *JETP Letters* **101** 719
11. Bogdanov O V, Pivovarov Yu L, Takabayashi, Tukhfatullin TA 2012 *J. Phys.: Conf. Ser.* **357** 012030
12. Takabayashi Y, Korotchenko, K B, Pivovarov Yu L, Tukhfatullin T A 2013 *Nucl. Instrum. & Methods* **B315** 105
13. Korotchenko K B, Pivovarov Y L and Takabayashi Y 2013 *Nucl. Instrum. & Methods* **B309** 25
14. Korotchenko K B, Pivovarov Yu L Takabayashi Y 2013 *Nucl. Instrum. & Methods* **B309** 25
15. Takabayashi Y, Pivovarov Yu L and Tukhfatullin T A 2014 *Phys. Lett.* **A378** 1520
16. Doyle P A and Turner P S 1968 *Acta Crystallogr.* **A24** 390
17. Kimball J C and Cue N 1985 *Physics Reports (Review Section of Physics Letters)* **125** 69